

Article

Locating Cave Entrances Using Lidar-Derived Local Relief Modeling

Holley Moyes ^{1,*} and Shane Montgomery ²

¹ Department of Anthropology and Heritage Studies, University of California, Merced, CA 95343, USA

² Cornerstone Environmental Consulting, Flagstaff, AZ 86001, USA; montgomery.shane.m@gmail.com

* Correspondence: hmoyes@ucmerced.edu; Tel.: +1-520-820-6748

Received: 12 December 2018; Accepted: 6 February 2019; Published: 20 February 2019



Abstract: Lidar (Light detection and ranging) scanning has revolutionized our ability to locate geographic features on the earth's surface, but there have been few studies that have addressed discovering caves using this technology. Almost all attempts to find caves using lidar imagery have focused on locating sinkholes that lead to underground cave systems. As archaeologists, our work in the Chiquibul Forest Reserve, a heavily forested area in western Belize, focuses on locating potential caves for investigation. Caves are an important part of Maya cultural heritage utilized by the ancient Maya people as ritual spaces. These sites contain large numbers of artifacts, architecture, and human remains, but are being looted at a rapid rate; therefore, our goal is to locate and investigate as many sites as possible during our field seasons. While some caves are entered via sinkholes, most are accessed via vertical cliff faces or are entered by dropping into small shafts. Using lidar-derived data, our goal was to locate and investigate not only sinkholes but other types of cave entrances using point cloud modeling. In this article, we describe our method for locating potential cave openings using local relief models that require only a working knowledge of relief visualization techniques. By using two pedestrian survey techniques, we confirmed a high rate of accuracy in locating cave entrances that varied in both size and morphology. Although 100% pedestrian survey coverage delivered the highest rate accuracy in cave detection, lidar image analyses proved to be expedient for meeting project goals when considering time and resource constraints.

Keywords: Lidar; GIS; Mesoamerica; Archaeology; Caves; Landscape; Ritual; Visualization; Maya; Belize; Sacred

1. Introduction

The ancient Maya civilization (250 AD–950 AD) of Central America developed and adapted to a tropical jungle environment that is the second largest continuous expanse of tropical forest in the world next to the Amazon Basin [1]. For archaeologists, the heavily forested terrain and thick understory has long plagued pedestrian surveys designed to locate and identify anthropogenic features and settlement traces across the landscape, rendering such studies time consuming and costly. Because of these challenges, Mayanists have long sought to use high-altitude imaging to map archaeological sites and settlements, beginning with aerial surveys by Charles Lindbergh [2] and advancing to satellite imagery [3,4]. Satellite imagery revolutionized landscape archaeology in areas that were not heavily forested revealing structures, roads, and extensive landscape modifications, such as raised fields, terracing, and buried features, as well as natural large-scale remnant features that were difficult to detect with pedestrian survey [5,6]. This has not only afforded discovery, but allowed archaeologists to monitor changes over time including heritage destruction [7,8]. However, these surveys had less impact on archaeologists working in tree-covered areas because the satellite or aerial imagery could not penetrate the forest canopies to the earth's surface. It is only with the advent of airborne light

detection and range (lidar) technology that we are now able to look “through” the trees and see the ground below at high resolution [9–16].

Lidar scans are carried out with instruments fitted to aircraft that emit pulses of light. In heavily forested terrain, some light will bounce off the canopy and vegetation, and some will rebound from the earth’s surface (ground returns), such that physical models of the ground surface may be derived from those points. The returned data are then classified and displayed as 3D point clouds and can be further manipulated to create relief models of the earth’s surface known as bare earth models. This enables researchers to locate both anthropogenic and natural landscape features over large areas that can be scanned in only a few days. Originally employed on a small scale in Europe [17], lidar-derived models are quickly becoming one of archaeology’s most important tools.

While most archaeologists concern themselves with both unmodified landscapes and anthropogenic features, such as buildings, terraces, and roadways, cave archaeologists are most interested in subterranean spaces. Caves are archaeologically important because they are often sheltered or protected from wind, water, or other erosional or taphonomic processes, and contain a wealth of information due to their excellent preservation and deep stratigraphic deposits [18–20]. For archaeologists working in the Americas, cave sites are critical to understanding religious practices [21,22]. Among many ancient Amerindians, caves were thought of as sacred features of the landscape and the homes of powerful deities, an essential feature of ancient cosmologies. As such, they were sanctified places to conduct rituals. Among the ancient Maya, ritual cave use dates to as early as 1200 BC [23], and sites continue to be used today by traditional Maya peoples [24,25]. These underground spaces are not only of interest to archaeologists, but research in caves is germane to other fields such as climatology, hydrology, terrain analyses, and biological studies.

What exactly is a cave? Definitions are typically dependent on human interaction. For instance, in the Encyclopedia of Caves, they are described as “a natural opening in the Earth, large enough to admit a human being [26]. Similarly, in the Encyclopedia of Cave and Karst Science, the term is applied to “natural openings, usually in rocks, that are large enough for human entry.” [27]. This non-specific term has come to mean any cavity in the earth and ontologically they are holes. There are three basic types of holes [28]: superficial hollows dependent on surfaces (that can include rockshelters, shallow, and deep caves with single entrances), perforating tunnels through which a string can pass (caves with multiple entrances), and internal cavities like holes in Swiss cheese, which are dependent on three-dimensional objects and have no contact with the outside environment (that could include caves that are closed off either naturally or anthropogenically).

In remotely sensed data, it is not possible to locate caves, but rather researchers seek to locate cave openings. This creates a challenge because the openings come in many shapes and sizes, can be horizontal or vertically aligned, and may be occluded by rock outcroppings [29]. Attempts to locate these sites have employed airborne infrared thermal scanners to identify thermal variation around potential openings [30,31], while other endeavors used multispectral scans and electromagnetic sensors to distinguish possible anomalies associated with karstic features [32,33]. These techniques were hindered by coarse resolution or issues arising from variables such as vegetation cover or atmospheric processes.

Lidar imagery has proven more successful, but most research has focused on locating sinkholes using automated techniques [34–40]. Sinkholes, located in karstic landscapes, are closed depressions in the earth’s surface with internal drainage caused by subsurface dissolution of soluble bedrock [36]. Because they can be quite large, they are more easily viewed using remote sensing techniques. The impetus for most research in locating sinks is that these features may collapse as water tables drop, creating hazardous conditions and property damage. Few researchers have attempted to locate caves associated with sinkholes but there are some notable exceptions. For instance, Weishampel and his colleagues [38], investigating the karstic features in western Belize, were able to detect sinkholes and vertical shafts with diameters of over 5 m. However, this study omitted smaller shafts, and inflow and exurgence systems, as well as horizontally accessed caves.

Yet, the caves of interest for archaeologists are often those with horizontal entrances that could be accessed without specialized equipment. While ancient people could build ladders or supply other means for entering vertical shafts, archaeological studies suggest that these were not the preferred venues for ritual activities [29]. Sinkholes can be quite deep and difficult to access, so typically, ancient people rarely used deep sinks; therefore, for archaeologists these locations are not necessarily desired targets. Sinkhole shafts are not only difficult to access, but they frequently contain “bad air” (high levels of CO₂), causing difficulty in breathing and rendering them potentially deadly. Additionally, for our purposes, many caves in Mesoamerica were host to large groups of ritual participants, and public access would have been a necessity in the ceremonial planning process, favoring horizontal entrances. While caves with smaller narrower openings were likely to have hosted rites that were smaller or more private with fewer participants, our research suggests that they would still have favored horizontal entrances with easier access.

Furthermore, for archaeologists, caves with smaller entrances are desirable targets because they are less likely to have been discovered by looters sustaining less damage to archaeological deposits and retaining a more complete artifact record. Typically, archaeological discovery of cave sites has depended on pedestrian survey or taking a “gumshoe” approach in which local people escort archaeologists to known sites. Once sites are discovered, they are by nature of their discovery disturbed simply by entry, whether by local people or researchers. In Mesoamerica, votive offerings left by ancient people in caves most often manifest as surface deposits that are particularly vulnerable to theft, looting, and vandalism. It is extremely rare for researchers to be the first to visit these sites. Therefore, artifact theft and movement, feature damage, and the disturbance of subsurface deposits is assumed in most cave contexts. Of the 82 caves in Belize investigated by the Belize Cave Research Project (BCRP), few had been spared by looters. There are only three known intact caves in western Belize: Actun Tunichil Muknal (Cave of the Crystal Sepulcher), discovered by geologist Tom Miller in 1989 and investigated by the Western Belize Regional Cave project in the mid-1990s [41,42]; Chechem Ha Cave (Poisonwood Water), a cave with a blocked entrance discovered by a local family who curated the site for tourist development [43]; and Ch'en Pi'x (Cave of the Awakening), a cave with a difficult entrance drop discovered by geologist Phillip Reeder and his crew [44].

There are a few ways that archaeologists can counteract this sort of heritage destruction. Public education is vital, but is a long-term process, whereas looting is occurring at a rapid rate as populations move into forested areas. Due to their remote locations, it would be difficult to protect even gated caves that could be easily broken into. Another complication is that many cave entrances are too large to be gated. Archaeological projects strive to record sites in their current conditions, but most caves must be considered “salvage” operations and we must acknowledge the incompleteness of the archaeological record [23]. Locating caves using lidar-derived models will potentially mitigate this problem by presenting an effective method for the discovery of sites so that they can be recorded, and research undertaken prior to looting.

In this paper, we present a methodology to locate potential caves sites by employing aerial lidar-derived point clouds. To analyze the lidar data, we use local relief models that require only a cursory knowledge of relief visualization techniques and no specialized skills in computer programming. We take a hybrid approach engaging both automation and manual evaluation, which has proved effective in discovering promising potentialities [29]. In our systematic study, we have been able to effectively predict locations of sink and horizontal cave entrances with fissure openings as small as 1 m in height. We begin by describing the area of our study's concentration, proceed to illustrate typological categories of cave openings, illustrate our methodologies and testing protocols, and discuss our results.

Setting: Geology and Karstic Background

Our survey area surrounds the site of Las Cuevas, a small to medium-sized ancient Maya pilgrimage center [45], located in Belize, Central America (Figure 1). The site has been under

investigation by the Las Cuevas Archaeological Reconnaissance (LCAR) project, directed by Holley Moyes, since 2011. The central site core consists of 26 structures organized on an east/west axis facing two plazas (Figure 2). The architectural features surround a dry sinkhole that leads to the entrance of an extensive cave system running beneath the buildings. Archaeologists know little about settlement surrounding pilgrimage centers in the archeological record or their underlying economies; therefore, the current phase of the LCAR project seeks to better understand settlement patterns and ritual landscapes surrounding the site core [29]. Among the ancient Maya, ritual landscapes can include caves, mountains, and water features, but our study focuses on ritual cave sites and their surrounds, employing both lidar imagery and pedestrian survey to identity natural and cultural features. Although many caves were used by the ancient Maya, not all caves show evidence of human activity. Our research on ritual landscapes investigates why some caves were used and others were not by studying cave morphology, spatial patterning over the landscape, and proximity to surface sites. To do this, we look at both utilized and vacant cave sites; therefore, the goal of our survey work is to find all caves across the landscape, not just the ones that show evidence of ancient Maya ritual use.

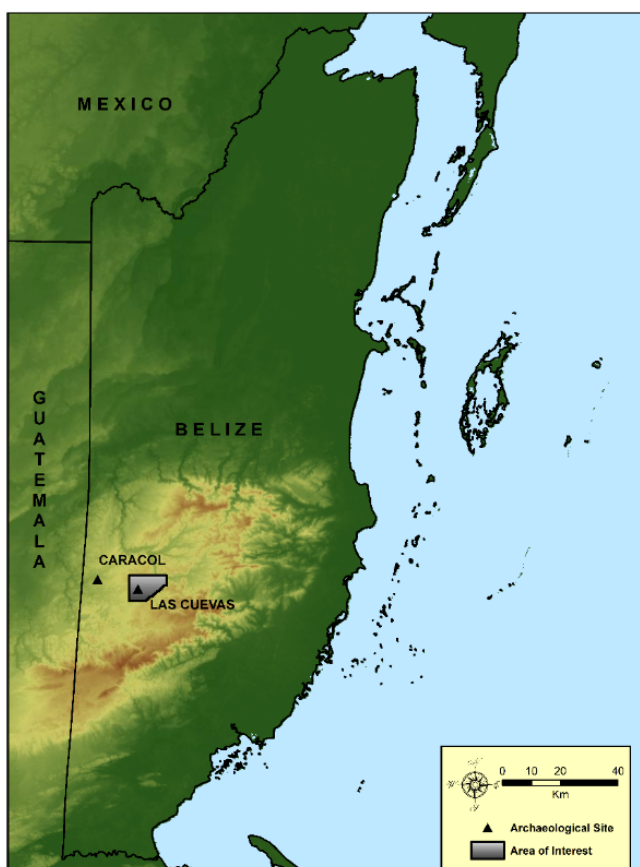


Figure 1. Belize map illustrates location of project area within the Chiquibul Forest Reserve.

The Las Cuevas site resides within the present-day Chiquibul Forest Reserve in western Belize near the southeastern extent of the Vaca Plateau (Figure 3), an area of protected land covered by tropical evergreen broadleaf forest [46] (Figure 4). Much of the Vaca Plateau falls within a geologic zone of Cretaceous limestone, with older Paleozoic layers found further west of the site and metamorphic and granitic material located within the Maya Mountains, 20 km to the north [46,47]. Covering more than 1000 km² [48], the Vaca Plateau extends east from Guatemala to the Maya Mountains, north to the boundary fault of the Belize River Valley, and south to the gorge of the Chiquibul River. Speleogenesis (cave origin and development) within the Vaca Plateau is associated with structural weaknesses in carbonate breccia derived from the Upper Cretaceous Campur Formation [49].

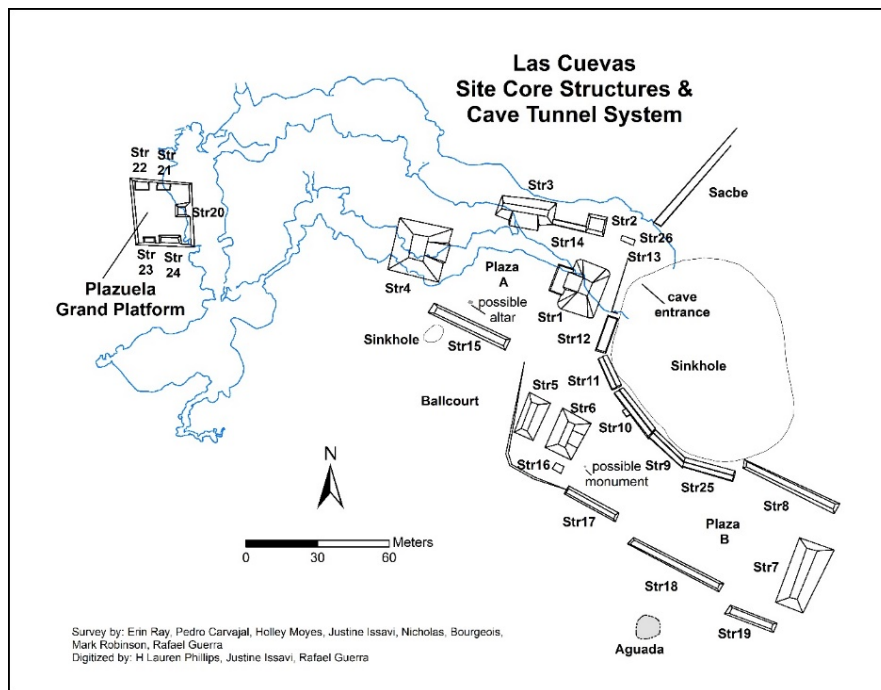


Figure 2. Map of Las Cuevas site illustrating cave system running beneath surface architecture (image courtesy of LCAR).

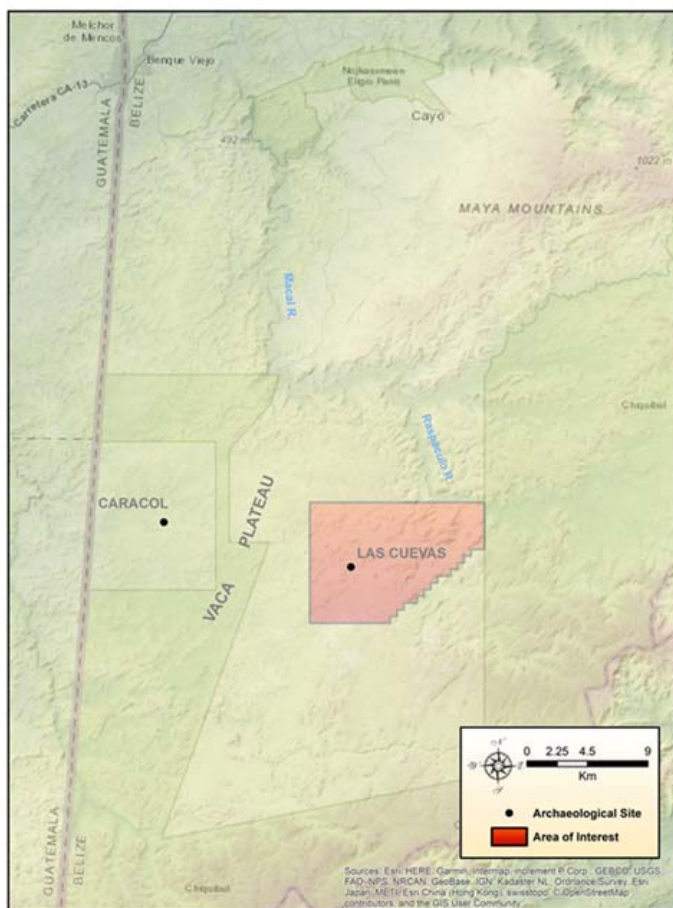


Figure 3. Regional map of Vaca Plateau illustrating location of Las Cuevas site and lidar coverage.

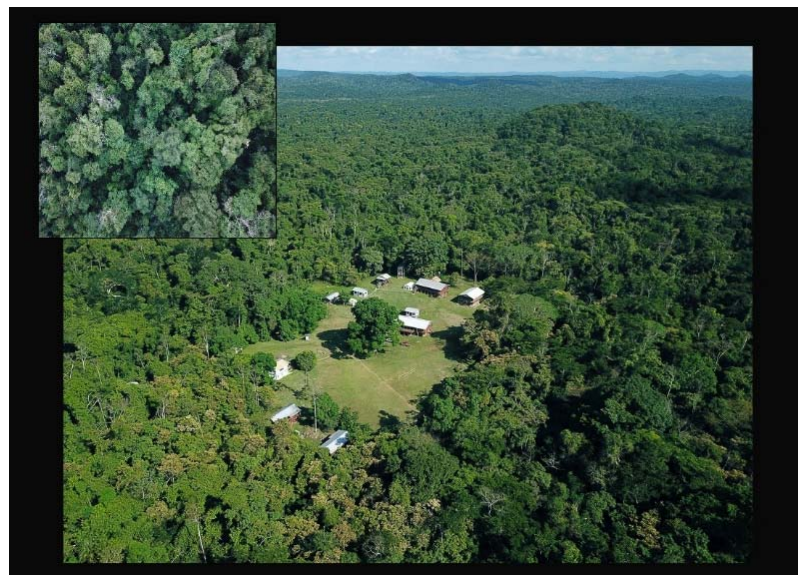


Figure 4. Aerial view of Las Cuevas site and research station in Chiquibul Forest Reserve. Inset shows view from above the tree canopy (images courtesy of LCAR).

In the vicinity of Las Cuevas, prevalent karst features include expansive sinkholes (dolines), restricted shafts and fissures, inflow and exurgence (outflow) caves, rock shelters, isolated phreatic caves formed by dissolution, and solution scarps (escarpments created by erosional undercutting). Through-flowing trunk conduits produced by surface stream penetration are rare compared to the extreme south of the Vaca Plateau, where the Chiquibul System forms the largest known hydrologically linked cave network in Central America [50]. The lack of conduits and the less dissected nature of the Las Cuevas area relate to the severe incising of the Macal and Raspaculo rivers to the east, which cut 200–300 m into the limestone, dropping the water table and preventing the formation of significant surface drainages on the plateau above [48].

Previous research indicates that many of the cave entrances detected within the Vaca Plateau are vertical, situated on sinkhole bottoms, hilltops, and the sides of residual hillslopes [51,52]. Shelter caves and shallow rock shelters are most common in association with solution scarps or at the bases of residual hill slopes. Likewise, inflow and exurgence caves appear at the margin between hill slopes and valley bottoms, where stream flow has penetrated the limestone. Some morphologically complex systems exhibit a combination of entrance types, illustrating the evolution of the formation processes.

The goal of our project is to locate not only sinkholes and vertical drops, but horizontal entrances as well. Caves with exclusively horizontal access occur mainly on side slopes at elevations of 50–150 m above existing dry valley bottoms. For our purposes, we classified cave entrances by size and morphology [29]. Horizontal entrances are large (>5 m in width and over 2 m in height), medium (1–5 m in width and 1–2 m in height), small (<1 m in width and >1 m in height), and fissures (<1 m in height with varying width) (Figure 5). Vertical entrances necessitate down climbs or technical drops. They come in a variety of forms (cylindrical, conical, bowl, or pan-shaped) and can be quite small or may measure hundreds of meters across and tens of meters in depth [53,54], may contain water or be filled in with sediment. Sinkholes and shafts were classified by the maximum width of the diameter of the opening as small manhole-like entrances (<1–5 m), medium (<5–10 m), and large (<10 m). Sinkholes containing horizontal cave entrances at their base were noted.

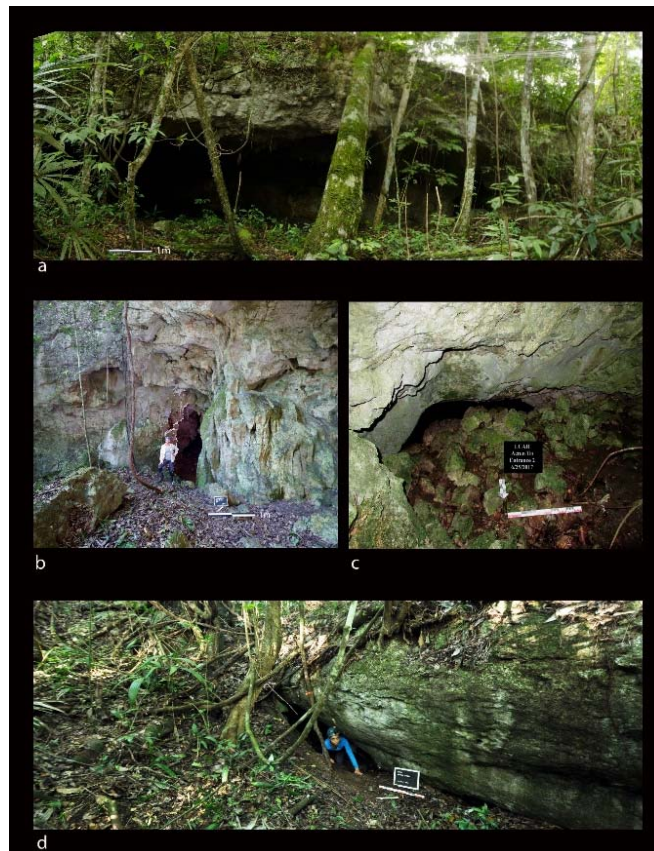


Figure 5. Horizontal cave entrances: (a) large entrance, Bird Tower Cave; (b) medium-sized entrance, Eduardo Quiroz Cave; (c) small entrance, Actun Uo (Uo Frog Cave); and (d) fissure entrance, Actun Z'uhuy Ch'en (Untouched Cave). (Photos courtesy of LCAR).

2. Methods

The Las Cuevas regional dataset was obtained in spring 2013 through the Western Belize lidar Consortium initiative, representing a cooperative effort between multiple archaeologists working within the country. The collection area covered approximately 1057 km² in western Belize, including much of the Belize River Valley and Vaca Plateau. Lidar acquisition was performed by the National Center for Airborne Laser Mapping (NCALM) over fourteen successive flights. An Optech Gemini Airborne Laser Terrain Mapper (ALTM, manufacturer, city, state abbreviation if in US or Canada, country) capable of 5 to 10 cm (2 to 4 in) vertical accuracy was mounted on a Cessna 337 Skymaster aircraft and flown at an altitude of 600 m above ground level with a ground speed of 60 m/s. The 325 survey lines were 137 m apart, resulting in a 300 percent swath overlap. The laser had a pulse rate of 125 kHz, a scan frequency of 55 Hz, and a scan angle of 18 degrees, resulting in a density of 15 points per square meter averaged throughout the entire area of interest [11,12]. Within the Las Cuevas lidar set, ground point returns ranged from 0.1 to 10 points per square meter based on associated canopy density and topography (Figure 6). Higher ground point returns were correlated with steep slopes, ridge tops, and modern infrastructure, while lower returns were found in low-lying *bajo* areas with thicker middle-level vegetation.

Point clouds were created from arrays of reflected light pulses emitted from the ALTM. In addition to flat or gently undulating terrain, vertical or steeply sloped terrain was captured within certain limits due to the scan angle (Figure 7). The entire point cloud represented the totality of pulse returns from upper canopy, understory, objects, and ground floor. The ground returns were classified by NCALM with automated methods utilizing TerraSolid Software and rendered to produce bare earth digital elevation models (DEMs) for further analysis of the natural and anthropogenic features.

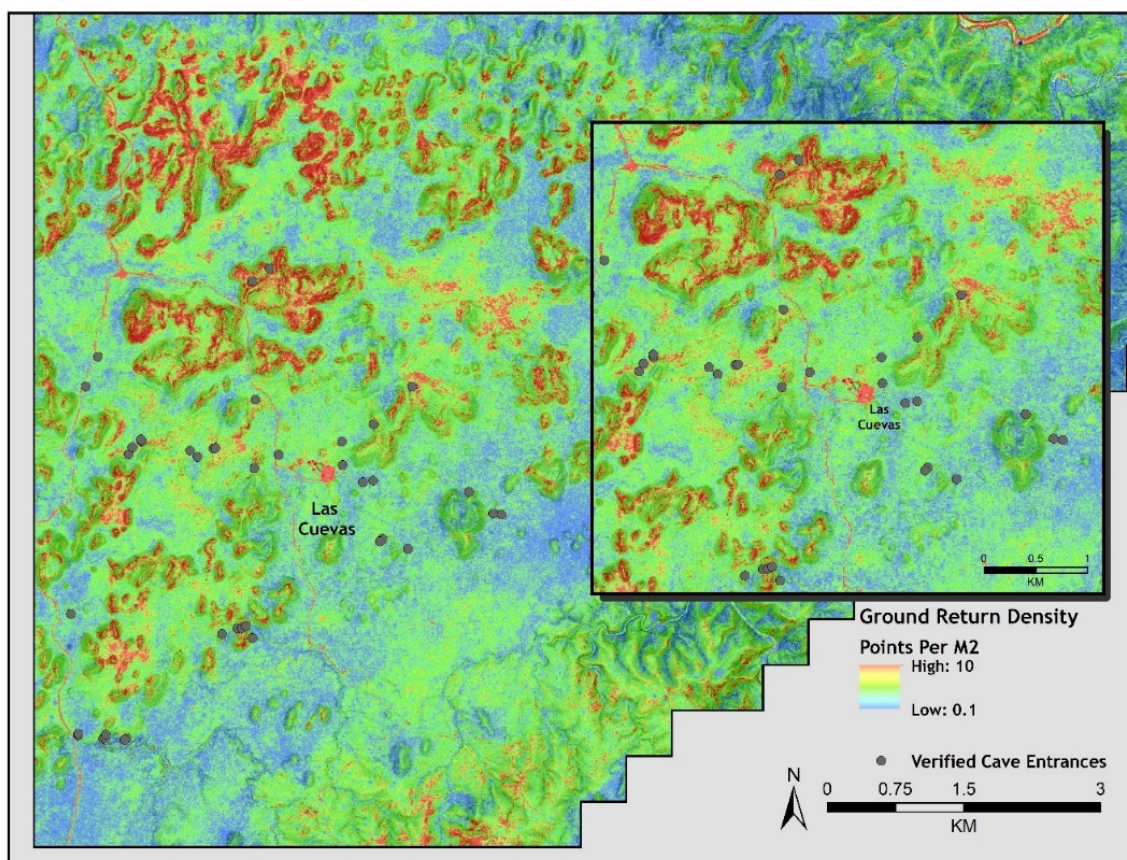


Figure 6. Map illustrating the density of LiDAR ground point returns correlated with topography.

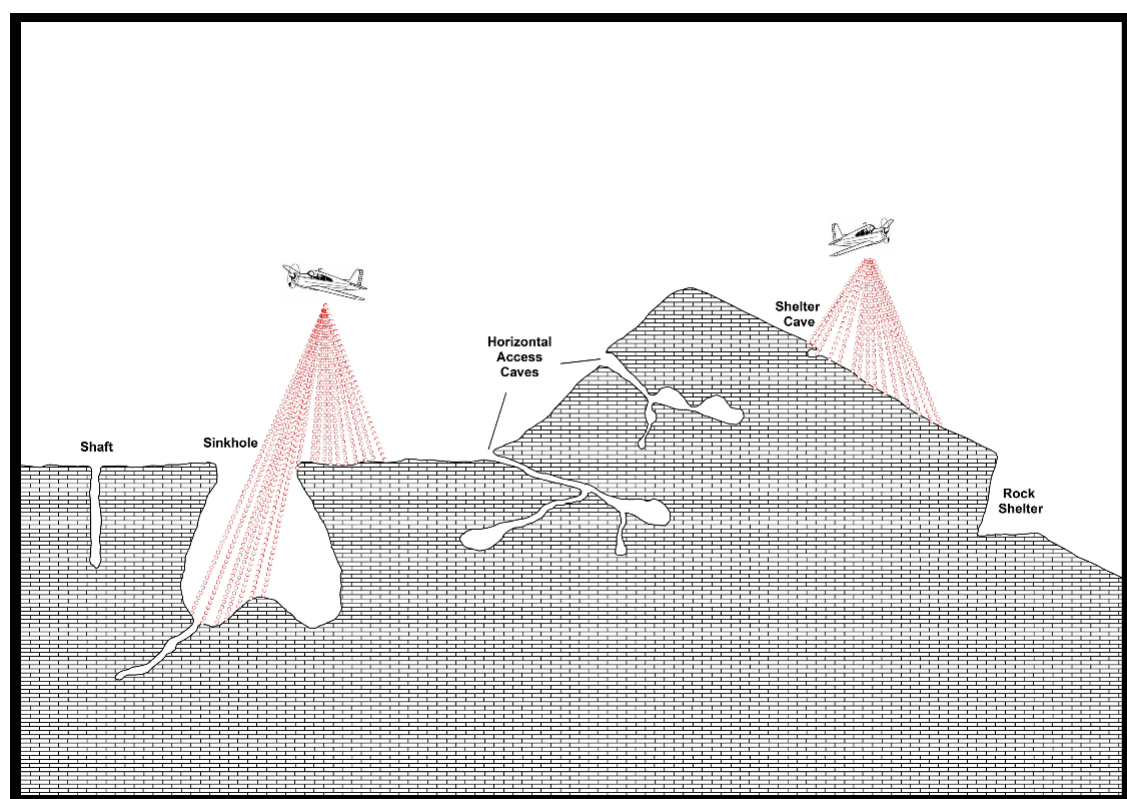


Figure 7. Schematic of lidar pulse angles (image by Shane Montgomery).

Data derived from lidar scanning, on the most basic level, contains X-, Y-, and Z-coordinates. Lidar data can be stored in a number of different formats, such as ASCII (text), binary, and LASer (LAS) format. LAS format has been endorsed by the ASPRS (American Society for Photogrammetry and Remote Sensing) [55] and was utilized for the Western Belize Lidar Consortium data. In addition to the spatial coordinates, the LAS files contained point classification, pulse intensity, RGB value, return number, scan angle, and overlap points. Once the lidar-derived DEM was created from this information, other relief visualizations and surface models were generated focusing on the detection of potential cave features.

Numerous raster data visualization techniques exist for the illumination of small-scale positive and negative relief features [56], including hillshade [57], sky-view factor [58], openness [59], local dominance [60], and local relief modeling (LRM). Each technique possesses strengths and weaknesses when applied to the task of remote cave detection. Hillshading has been widely utilized by archaeologists and other researchers for landscape recreations across diverse topographic settings. However, one disadvantage inherent within hillshading relates to its single illumination source, which can obscure individual features in shadow. Furthermore, hillshading is produced through cosine values based on the illumination and angle of the relief surface; the technique does not classify topographic change based on immediate variation and often oversaturates areas facing directly towards or away from the illumination source. Detection of these subtle elevation differences represents a crucial step in the documentation of all potential cave features across a given landscape.

After experimentation with multiple techniques, the project selected LRM for its ability to highlight both positive and negative anomalies in relation to the generalized landscape [56]. The method, when properly utilized, extracts human modifications and potential cave features on the immediate level and provides effective understanding of the associations between prehistoric constructions and ritual cave spaces. Although automated algorithms have been used to streamline sinkhole detection [37,61], manual methods are best employed in local relief modeling when attempting identification of the range of karstic features across a given landscape. Manual detection of potential cave features offers the user the ability to discern illusive entrance types (i.e., horizontal and inflow/exurgence caves) not readily captured by automated methods. Additionally, natural landforms displaying concave characteristics, such as restricted valley bottoms, appear as negative relief and would require purging before additional analyses [62].

Detection of potential cave entrances was conducted primarily through ArcMap and LP360. Raster creation and editing was performed within ArcMap version 10.3, while LP360 was used visualize point clouds in profile and 3D views [29]. An initial local relief model was created within ArcMap using the LRM Toolbox [63]; the LRM Toolbox ran the lidar-derived DEM through eight processing steps designed to extract minor variations in elevation based on overall trends within the larger surrounding landscape (Figure 8). A circular neighborhood radius of 25 m was established for the kernel standard size based on the presumed maximum extent of possible sinkhole openings within the Vaca Plateau [48]; this kernel size has been utilized in previous landscape modeling research on similar gradually sloping terrain with positive results [56,62].

Once initial processing was complete, the 222 km² Las Cuevas LRM was draped over a slope model produced from the original lidar-derived DEM and divided into 500 m × 500 m tiles to correspond with the LAS point cloud grid size previously established by NCALM. Alphanumeric designations were given to each grid tile to provide a unique identification number to each remotely detected cave entrance or karstic feature. Negative topographic anomalies were identified within each grid through LRM index value analysis and then compared to the existing hillshade layer provided by NCALM. Spatial and morphological characteristics of potential cave entrances were explored through a combination of manual visualization of point cloud data within LP360 and semi-automated LRM analysis within ArcMap. Features of interest were examined in profile (Figure 9) and 3D views of all points classified as ground returns in order to generate data on entrance width/height and maximum depth. Identified negative anomalies were classified based on morphology (horizontally or vertically

accessed) and topographic setting (i.e., slope, valley, hill top). These potential cave entrances were then plotted onto the existing slope model for further analysis and uploaded to handheld GPS devices for field verification.

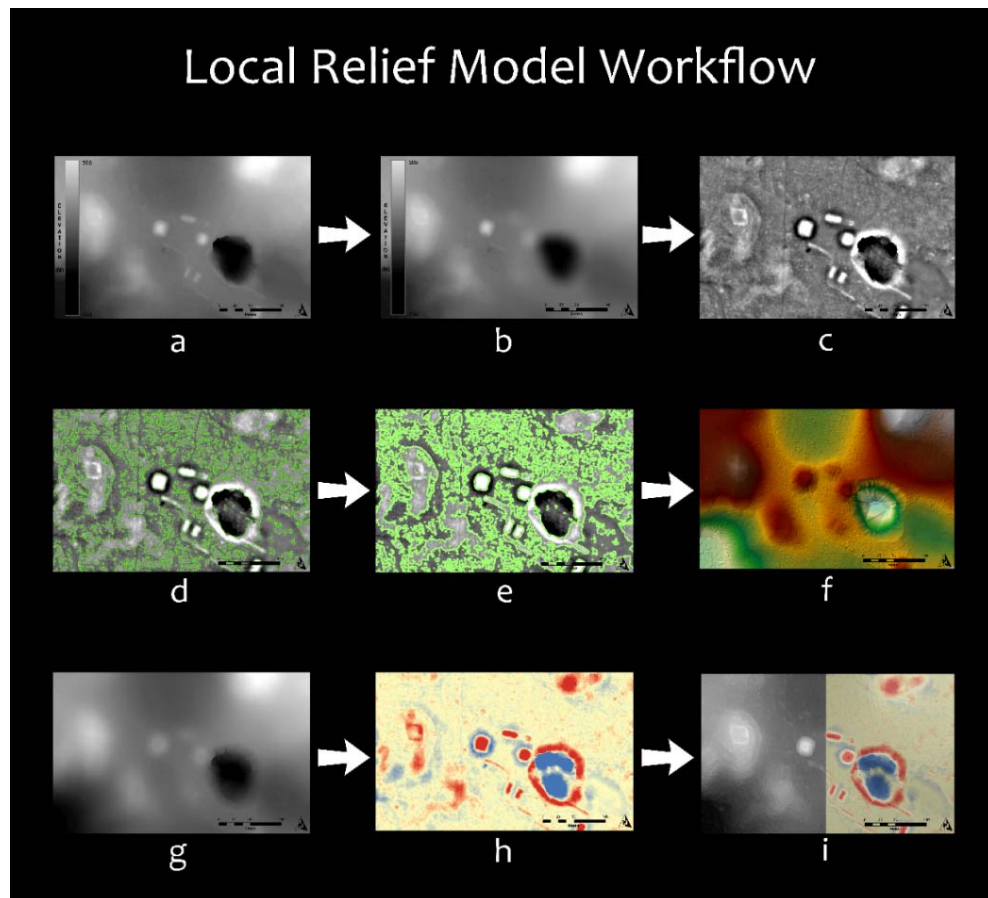


Figure 8. LRM Workflow Chart: (a) original 1-m DEM of Las Cuevas, (b) split image of original DEM and smoothed DEM, (c) difference of smoothed and original DEM, (d) creation of contour lines, (e) contours converted to elevation points, (f) Triangulated irregular network(TIN) created from elevation points, (g) Digital terrain model (DTM) generated from TIN, (h) LRM created from subtraction of DTM from original DEM, and (i) split image of original DEM and LRM.

Analysis of Remotely Detected Cave Entrances

Research conducted on our lidar coverage [29] identified 377 remotely sensed cave entrances within the 222 km² zone encapsulating a significant portion of the southeastern Vaca Plateau. Due to the size of the data set, we chose to narrow the project's focus to a 95.25 km² region representing the maximum extent of the prehistoric settlement zone of Las Cuevas. The updated study area contained approximately 42% ($n = 157$) of all formerly identified remotely sensed cave entrances (Figure 10).

Analyses of the lidar data suggested that closed depression sinkholes were the most commonly encountered cave entrance type within the sample, accounting for 66% ($n = 104$) of all remotely detected features. The morphology of these sinkholes was easily visualized in cross-section, with multiple returns located below the presumed ground level. Vertical shafts with openings less than one meter were rare throughout the study area ($n = 3$; 3%) and over half of the lidar-detected sinkholes displayed small openings between 1.1–5 m ($n = 55$; 53%) (Figure 11a). Medium-sized sinkholes with openings between 5.1–10 m comprised 31.7% of the closed depressions ($n = 33$). Sinkholes with diameters exceeding 10 m were infrequently encountered within the Las Cuevas study area, consisting of 12.5% ($n = 13$) of the doline features. Sinkhole depths ranged from 1.3–30 m, with an average negative relief

of 5.7 m. The Las Cuevas central site core is built around a large sinkhole that measures 85 m with a depth ranging from 13–15 m. The cave entrance is 9 m in height and can be observed in profiles view in the lidar imagery (Figure 11b). The second largest sinkhole in the Las Cuevas region, Actun P'ook, measures 60 m across, and along with Las Cuevas is considered an outlier in this portion of the Vaca Plateau (Figure 12).

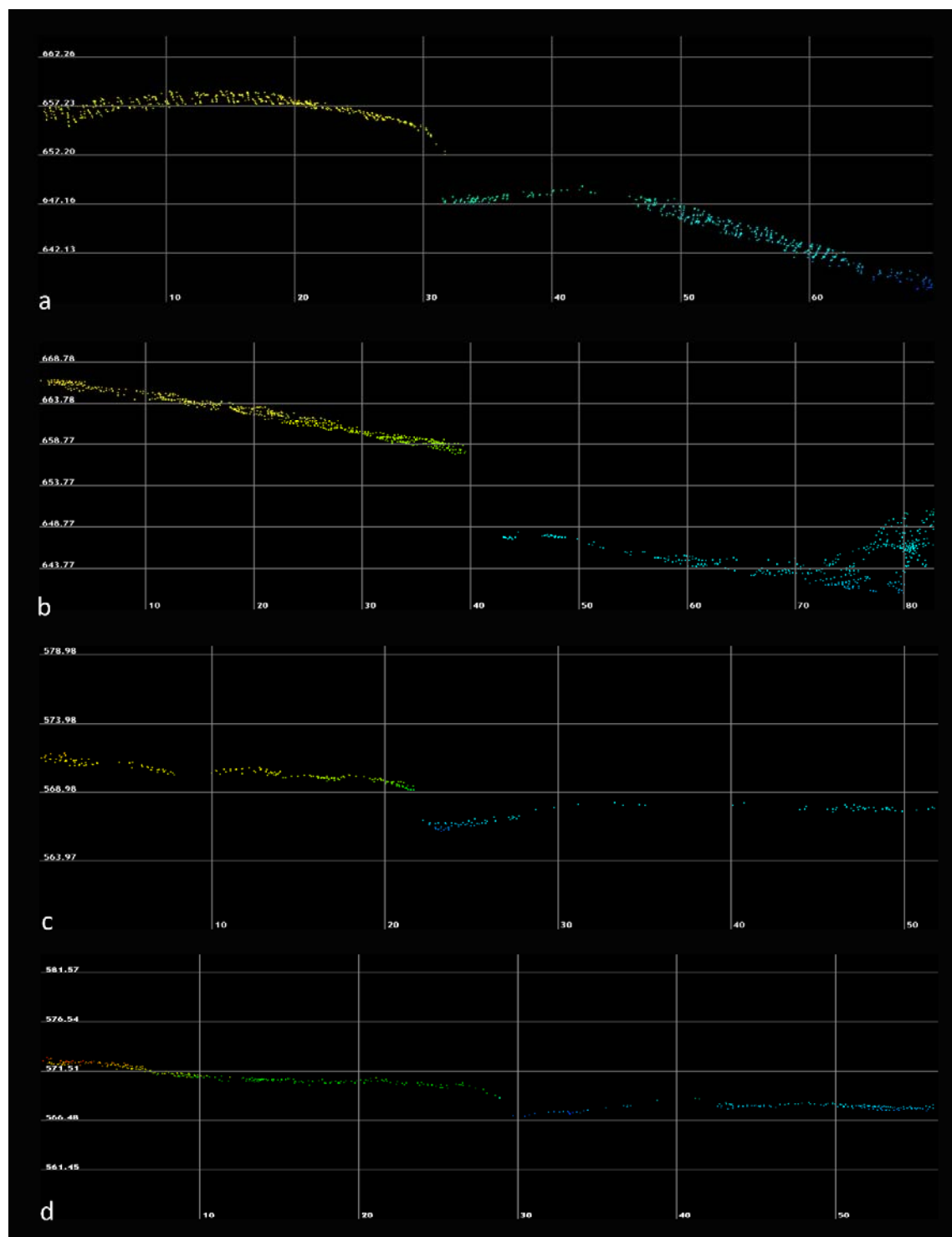


Figure 9. Point cloud profile images of four horizontal cave entrances rendered in LP360: (a) large entrance, Bird Tower Cave; (b) medium-sized entrance, Eduardo Quiroz Cave; (c) small entrance, Actun Uo (Uo Frog Cave); and (d) fissure entrance, Actun Z'uhuy Ch'en (Untouched Cave).

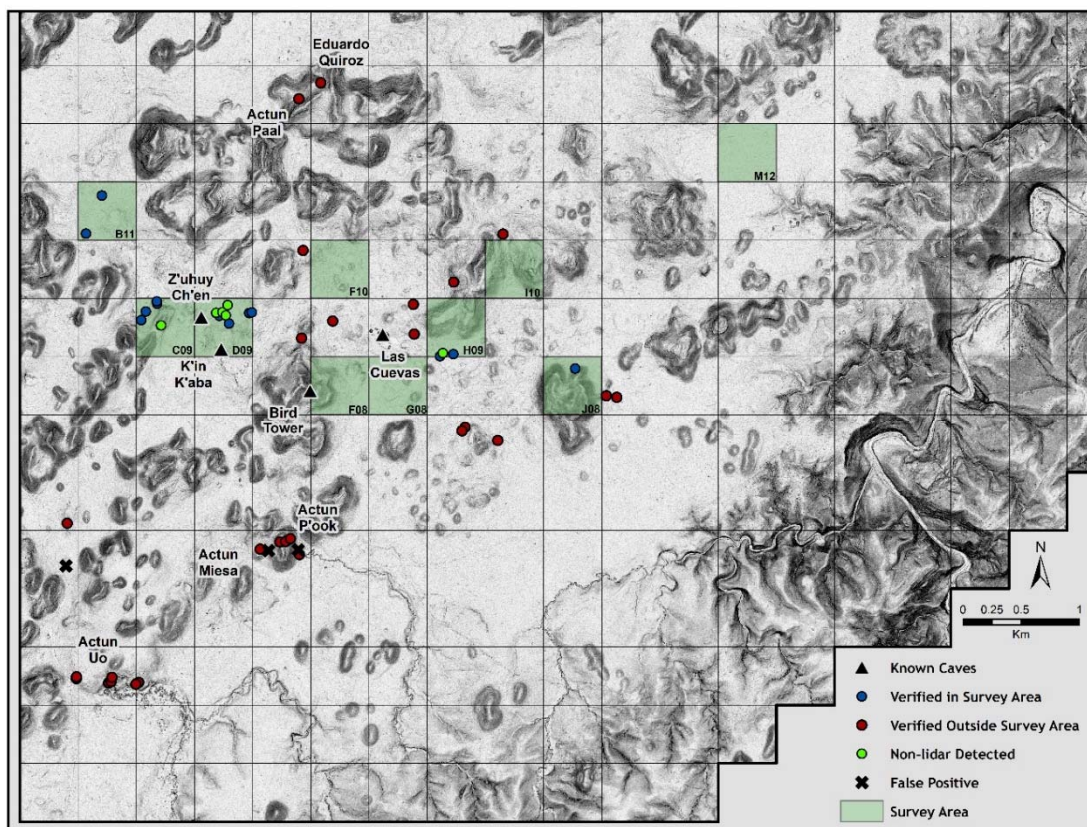


Figure 10. Map of pedestrian survey area for 2017/2018 field seasons. Green tiles indicate area systematically surveyed.

Horizontally accessed caves accounted for 28% ($n = 44$) of the remotely detected features. Caves of this type were less obvious when viewed in cross-section compared to the more common sinkhole features, and care was taken to differentiate between cliff faces and genuine horizontal entrances. In profile, sheer cliffs retained ground points and were associated with slopes angling away from the exposure. By contrast, potential horizontally accessed caves lacked ground returns in the void between the entrance ceiling and base. Furthermore, many examples displayed sloped areas angling towards the entrance, indicating movement of colluvial soils into the cave opening. Estimated entrance heights ranged from 1.8 to 16.6 m, with an average clearance of 4.7 m. Excluding one previously known cave (Z'uhuy Ch'en or Pure Cave) with a fissure entrance less than 1 m in height, no other horizontally accessed fissure entrances were detected within the study area. Fourteen caves classified with horizontal access (31.8%) display estimated entrance heights of less than 3 m; an additional 15 horizontally accessed caves (34.1%) featured clearances between 3.3 and 5 m. The remaining 15 entrances within the classification measure between 5.3–16.6 m in height. Within the sample, horizontal width ranged between 1.2 and 17.5 m.

The remaining remotely sensed features consisted of caves associated with drainage inflows and exsurges (Figure 13). Eight inflow caves were identified within the Las Cuevas study area, all displaying horizontally accessed entrances. A majority of these entrances ($n = 6$; 75%) were small to medium in height and opening, with only two examples exceeding 5 m tall and 4.5 m in width. A single exurgence cave was detected on an unnamed tributary of the Monkey Tail Branch, displaying a 5.5-m-wide opening and an estimated entrance of 12.6 m. No through-flowing trunk conduits were identified within the study area.

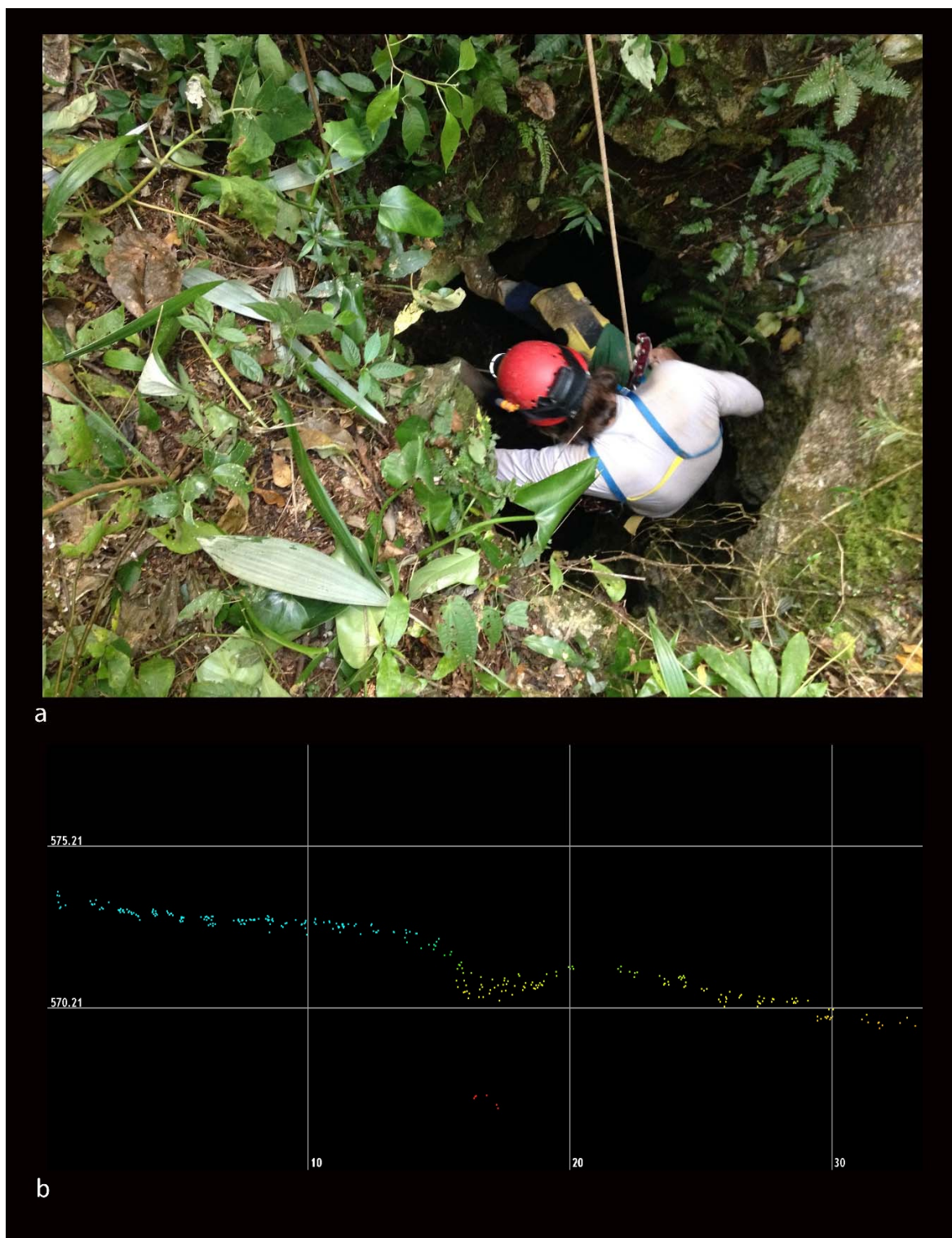


Figure 11. Photo of small shaft opening (**a**). (Matt Oliphant pictured in opening (top), Photo courtesy of LCAR), (**b**) and lidar point cloud in profile using LP360.

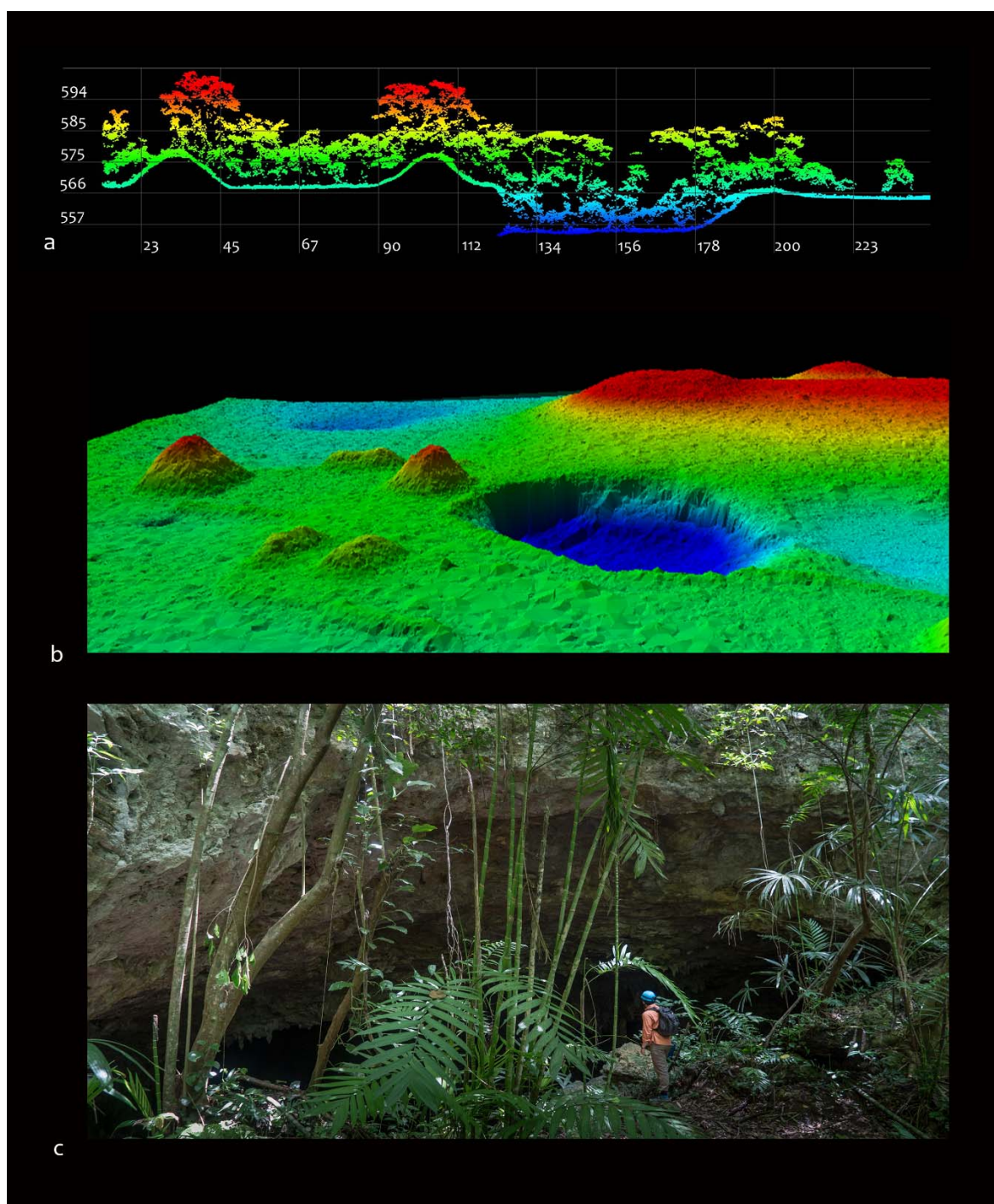


Figure 12. Las Cuevas surface site and sink hole: (a) point cloud of cave and sinkhole viewed from the north using LP360, (b) 3D image of sinkhole and surface structures (LP360), (c) photo of large Las Cuevas cave entrance (courtesy of LCAR).

Analysis of the topographic setting of all remotely detected cave entrances within the study area indicated that a majority of all features occur on hill slopes ($n = 57$, 42.7%), with a lower percentage ($n = 55$, 35%) situated within flat or gently undulating valleys. Potential cave entrances were less common along slope bases ($n = 21$, 13.4%) and within larger shallow depressions ($n = 6$, 3.8%). Seven remotely detected cave entrances (4.5%), exclusively minor sinkhole features, had been incorporated into ancient Maya agricultural terracing. Only one karstic feature, Actun P'ook,

was located at the apex of a ridge. The distribution of karstic features within the Las Cuevas region illustrates the diverse formation of cave systems within this portion of the Vaca Plateau.

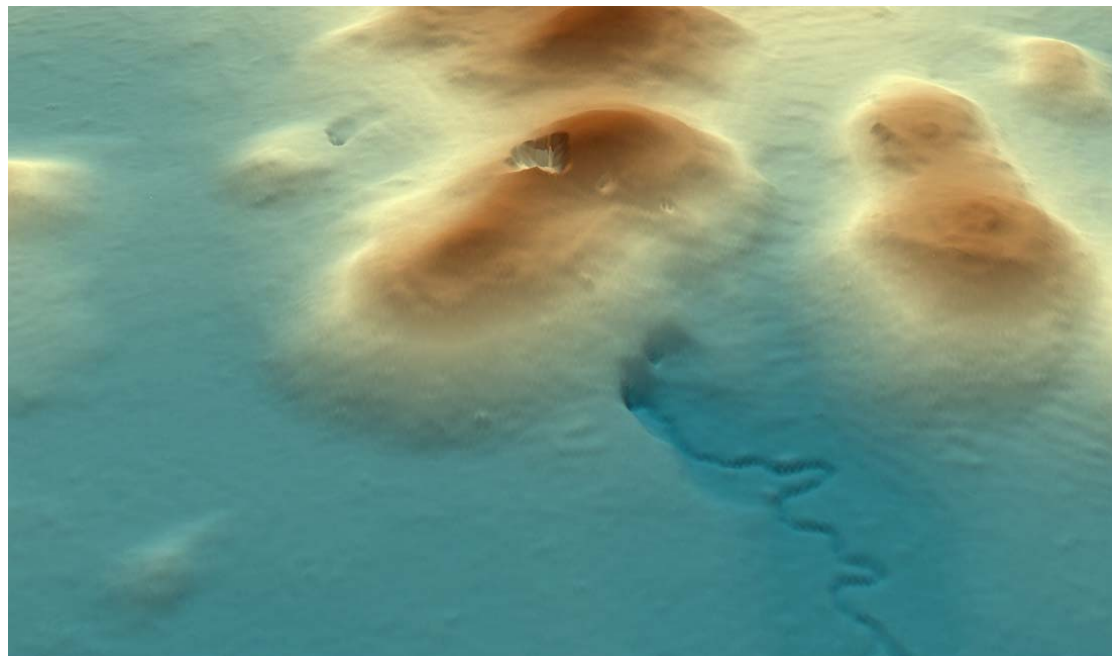


Figure 13. Lidar image showing drainage inflow indicating the presence of a cave entrance (Actun P'ook or Sombrero Cave).

Before our lidar survey, the project was aware of four known caves in the 95.25 km^2 survey area: the cave at Las Cuevas (large sink with horizontal entrance), Bird Tower Cave (large sink with horizontal entrance), K'in Kaba (large horizontal entrance with two openings), Zuhuy Ch'en (fissure entrance). The lidar images suggested that there were many more potential cave sites and possibly large cave systems in the project area. However, despite advanced technology, the accuracy and validity of remotely detected data remained in question, particularly regarding sub-surface features. We expected to find two types of errors: false positives (anomalies in the lidar images that resembled cave openings), and cave openings that went undetected in the lidar visualizations.

To test our findings, we used two methods of survey, each designed to uncover different types of errors and that would help to correlate features in the imagery and those on the ground. First, we directed an opportunistic survey (Survey 1) to verify select caves identified on the lidar. In this method, we directly visited potential cave openings based on the lidar imagery. This method would help to ferret out false positives and help us to calibrate our interpretations with real-world data. In Survey 2 we conducted a systematic pedestrian survey within 10 dispersed grids around the Las Cuevas site center. The grids were located in various terrains including bajos (low-lying swamps and low hills) (B11, F10, G08, M12), karstic ridges, hills, and valleys (C09, D09, F08, H09), and steep slopes (J08, I10). The aim of this method was to obtain total coverage of specified target areas to account for undetected openings, as well as false positives within the data set. This method was much more laborious and time consuming.

The systematic survey was completed over two six-week field seasons in the summers of 2017 and 2018 using two to three crews of three people each. The 95.25 km^2 survey area was divided into 381 contiguous $500 \text{ m} \times 500 \text{ m}$ tiles. Each potential cave entrance previously detected through remote analysis was provided an identification number based on an alphanumeric grid system (i.e., A03_C01). Only caves with moderate to heavy ancient Maya usage were given names by our Maya in-country partners. Ten tiles, a combined 2.5 km^2 were selected for systematic pedestrian survey comprising 2.6% of the target area. The objective in tile selection was to survey a variety of micro-landscapes and

topographies (such as hilly or flat, boggy vs. dry) to determine the active factors influencing lidar detection within the project area. By selecting a subset of the data, it was then possible to cover 100% of the terrain within the tile, assuring that no karstic features escaped observation.

The logistical goal of the Las Cuevas survey was to inspect targeted areas in a methodical fashion to document the totality of natural and anthropogenic features in a dense, dynamic sub-tropical forest environment. Traditional survey methods often employed in more open landscapes proved non-viable in the thick rainforests of the Vaca Plateau. Instead, a method more suitable to the environment was used. Within ArcMap, a fishnet grid was created for each tile consisting of 50-m lattices aligned to the cardinal directions. The fishnet, along with the remotely detected cave point data, were uploaded to Garmin 64s GPS units for each survey crew. Survey crews cut through vegetation to create paths along the 50-m spaced transect, stopping at each vertex and radiating outward counterclockwise in a 25-m arc, providing total coverage between each point.

3. Results

Of the 152 cave openings revealed in our lidar imagery, 29 (19%) were visited opportunistically in Survey 1 (Table 1). Of these, 26 (86%) proved to be cave openings or sinks, though some represented multiple entrances to the same cave system. For instance, Actun Uo (Uo Frog Cave) had five entrances, all of which were detected on the lidar image. Survey 1 located three false positives as well, which included one sheer limestone face that contained no rock shelter area or shelter cave (E05_C05), one depressed interior drain with dirt slopes (A05_C03), and one area of dead trees and thick vegetative growth incorrectly identified as a small horizontally accessed cave (E05_C07). Out of ten predicted horizontally accessed sites, we located eight actual entrances on pedestrian survey. Therefore, 70% of the predicted horizontal entrances were confirmed.

Table 1. Caves located in Survey 1 and Survey 2, and four previously known caves.

Survey 1—Cave Openings Surveyed Opportunistically								
Cave Name	Cave_ID	Cave_Type	Size	Max Width of Opening (m)	Max Sink Depth/Hor Ent Ht (m)	Topography	Verified	Artifacts Present
Actun Uo	B03_C02	Inflow_Drain	Small	0.7	1	Valley	Yes	No
Actun Uo	B03_C01	Inflow_Drain	Small	1.2	2	Valley	Yes	No
Actun Uo Ent 1	A03_C01	Hor Ent	Large	5	2.9	Depression	Yes	Yes
Actun Uo Ent 2	A03_C02	Hor Ent	Medium	2.8	2	Depression	Yes	Yes
Actun Uo Ent 3	B03_C03	Hor Ent	Large	7.8	7.4	Solution Scarp	Yes	Yes
Actun P'ook Ent 1	E05_C03	Hor Ent	Large	16	6.5	Side Slope	Yes	Yes
Actun P'ook Ent 2	E05_C02	Sink	Large	60	30	Hill Top	Yes	Yes
Actun P'ook Ent 3	E05_C04	Hor Ent	Medium	4.4	8	Side Slope	Yes	Yes
Actun P'ook Ent 4	E05_C06	Hor Inflow Drain	Large	14.2	11.5	Slope Base	Yes	Few
Actun Miesba	E05_C01	Sink-Hor Ent	Large	11.9	10	Side Slope	Yes	Yes
Actun Paal	E13_C01	Hor Ent	Medium	4.3	4	Side Slope	Yes	Yes
Eduardo Quiroz	F13_C01	Hor Ent	Large	6	7.4	Side Slope	Yes	Yes
Dinoaur Egg Cave	A06_C01	Inflow_Drain	Large	17	8.7	Valley	Yes	Yes
NA	I07_C01	Inflow_Drain	Medium	2.8	2.2	Slope Base	Yes	No
NA	K08_C02	Inflow_Drain	Small	1	0.5	Valley	Yes	No
NA	B03_C04	Sink	Large	11	2.5	Side Slope	Yes	No
NA	C03_C01	Sink	Large	17.5	7.2	Side Slope	Yes	No
NA	G09_C02	Sink	Small	1.5	3.2	Side Slope	Yes	Few
NA	H10_C01	Sink	Medium	6	5.8	Side Slope	Yes	No
NA	E09_C02	Sink	Medium	7.5	3	Valley	Yes	No
NA	E10_C02	Sink	Medium	5.2	7.7	Valley	Yes	No
NA	F09_C01	Sink	Small	4	3.3	Valley	Yes	No
NA	G09_C03	Sink	Medium	5.1	3.7	Depression	Yes	No
NA	H07_C01	Sink	Large	11.1	4.5	Valley	Yes	Few
NA	H07_C02	Sink	Large	23	4.3	Valley	Yes	No
NA	I11_C01	Sink	Small	2.9	2.9	Valley	Yes	No
NA	K08_C01	Hor Ent	Medium	3.3	3.5	Slope Base	Yes	No
NA	E05_C05	Hor Ent	Small	4.1	6.4	False Positive	Yes	No
NA	E05_C07	Hor ent	Small	3.6	2.5	False Positive	Yes	No
NA	A05_C03	Sink	Large	25	5.2	False Positive	Yes	No

Table 1. Cont.

Survey 2—Systematic Coverage of Survey Tiles								
Cave Name	Cave_ID	Cave_Type	Size	Max Width of Opening (m)	Max Sink Depth Hor Ent Ht (m)	Topography	Verified	Artifacts Present
NA	B11_C03	Shaft	Small	0.5	5.5	Valley	Yes	No
NA	J08_C01	Shaft	Small	1	2.3	Slope Base	Yes	No
NA	C09_C03	Sink	Small	2.4	3.9	Slope Base	Yes	No
NA	C09_C04	Sink	Small	2.5	2.2	Valley	Yes	No
NA	D09_C02	Sink	Medium	5.5	7.9	Valley	Yes	No
NA	D09_C04	Sink	Medium	6.8	5.4	Valley	Yes	No
NA	C09_C01	Sink	Medium	7.9	5.3	Valley	Yes	Few
NA	D09_C03	Sink	Medium	9.1	3.5	Valley	Yes	No
NA	B11_C01	Sink-Hor Ent	Large	10.5	10.5	Valley	Yes	Few
NA	H09_C02	Sink	Large	11.5	2	Valley	Yes	No
NA	H09_C01	Sink	Large	12	8	Valley	Yes	No
NA	D09_C05	Sink	Large	13	6.3	Valley	Yes	No
NA	C09_C02	Sink-Hor Ent	Large	15.2	12.5	Valley	Yes	Yes
Cave openings not detected by lidar								
NA	H09_T02	Sink	Small	1	6	Valley	Yes	No
NA	D09_T09.1	Sink	Small	2.1	3.3	Valley	Yes	Yes
NA	D09_T08	Sink	Small	2.7	0.9	Valley	Yes	No
NA	D09_T10	Sink	Small	4.4	0.5	Valley	Yes	No
NA	D09_T09.2	Sink	Medium	5	2	Valley	Yes	No
Actun Chichan	C09_T06	Horizontal Ent	Blocked Ent		Side Slope		Yes	Yes
Known caves prior to survey								
Las Cuevas	NA	Sink-Hor Ent	Large	85	14	Valley	Known	Yes
Bird Tower	NA	Horizontal Ent	Large	14.8	7.3	Side Slope	Known	Yes
K'in K'aba Ent 1	NA	Horizontal Ent	Large	17.3	4.5	Slope Base	Known	Yes
K'in K'aba Ent 2	NA	Horizontal Ent	Medium	5.1	3.5	Side Slope	Known	Yes
Z'uhuy Ch'en	NA	Horizontal Ent	Fissure	0.6	0.7	Slope Base	Known	Yes

Within our systematic Survey 2, 13 potential cave openings were found in 5 of the 10 tiles surveyed (B11, C09, D09, H09, J08). These consisted of medium to large-sized sinkholes ($n = 11$) and small constricted shafts ($n = 2$). Six caves within the tiles were not identified through remote sensing methods and were detected exclusively via pedestrian survey. These included three shallow sinkholes, one constricted shaft, one horizontally accessed cave, and one cave with a blocked entrance. Within the local relief model, the shallow sinks were largely indistinguishable from other minimal relief depressions across the project area, such as household reservoirs or chultuns (small underground storage areas carved into limestone bedrock). None of the three sinks exceeded two meters in depth. Similarly, the undetected shaft was situated within a slight depression ubiquitous throughout this portion of the Vaca Plateau. The actual shaft was obscured by a collection of palm fronds, further concealing the minor feature. The single horizontally accessed cave occurred in a clearing where massive hardwood trees had previously toppled, allowing sunlight into the lower near ground levels and leading to the growth of thick vines and grasses. Due to this thick low vegetation, few lidar points were able to penetrate to ground level, resulting in poor coverage. Finally, the blocked entrance, a small horizontally accessed cave, Actun Chichan (Small Cave), was almost completely infilled with limestone blocks and small boulders, giving no indication on the surface that would be remotely detectable. It is likely that the entrance was closed by the ancient Maya, though there were a few artifacts inside.

In areas in which our survey coverage was 100%, we found cave openings not detected in the lidar. This is the most common error reported by archaeologists when using lidar imagery to detect small low-lying structures (<2 m in height) in areas of dense low vegetation [29,64–67]. In other areas of Belize, notably the Belize River Valley, invasive Guinea grass and secondary-growth vegetation has limited the effectiveness of lidar in the identification of minor archaeological features [68]. In our survey area consisting primarily of high forest canopy, we were likely to encounter this error as a result of tree fall and rarely due to low-growth vegetation covering cave openings. False positives were few ($n = 3$) and were the result of steep slope angles or tree fall, but not correlated with vegetation types as reported in other archaeological studies [66,68–70]. Likewise, density of ground returns did not affect the overall detection of karstic features, even when potential sinkhole openings were denoted by a single anomalous return point. These findings indicate that within our survey area, only a small percentage

of cave entrances will escape detection due to human-constructed blockages or vegetative cover (see Figure 6 which illustrates the relationship between detected cave entrances and point cloud densities).

4. Discussion

After two years of field research, 39 newly identified, remotely sensed cave openings were confirmed and an additional six caves were encountered through pedestrian survey, greatly increasing both the number of known sites in the greater Las Cuevas area. Prior to the 2017 field season, the project located and investigated only four caves in the immediate area: the cave at Las Cuevas, Z’uhuy Ch’en (Pure Cave), K’in Kaba (Birthday Cave), and Bird Tower. These were either known caves or had been found by pedestrian survey. All four of these sites were visible within the local relief models, including the fissure entrance associated with Z’uhuy Ch’en (see Figure 9). Working with the lidar imagery was instrumental in increasing the number of known sites from 4 to 45.

Combined, 25% of the 157 potential cave openings within the projected area were verified over two summer field sessions. The 39 confirmed cave entrances led to the identification of 15 fully or partially developed cave systems (37.5%). Actun Uo (Uo Frog Cave), Actun P’ook (Sombrero Cave), Eduardo Quiroz, Actun Paal (Child’s Cave), Actun Miesa (Nothing Cave), and one unnamed cave (C09-C02) had moderate to heavy prehistoric use ($n = 6$), and four others showed minimal use. Three of the remaining systems remain underexplored due to technical requirements (i.e., climbing gear) or bad air. Prehistoric use by the ancient Maya within smaller sinks and shafts was scant, often denoted by low quantities of ceramic material. The morphology of the features rendered them difficult to access without the aid of ropes or ladders, and organic matter and the lack of secondary entrances impeded ventilation in many of these systems. High levels of carbon dioxide were registered in chambers associated with these openings, which would have proven dangerous and potentially fatal to past populations attempting any prolonged ritual activities.

Although horizontally accessed caves were more difficult to detect, local relief modeling and ground-truthing revealed a strong correlation between remotely-sensed entrances and developed cave systems. Two caves in particular proved heavily utilized in prehistory. Actun Uo (Uo Frog Cave), located four kilometers southwest of Las Cuevas, featured three horizontal entrances, numerous chambers and passages, and a through-flowing subterranean stream. The cave was architecturally modified by the ancient Maya, who constructed multiple platforms, partitions, standing stone-altar complexes, and enclosed masonry rooms throughout the system. Eduardo Quiroz Cave, a previously identified system excavated more than half a century ago by A.H. Anderson and David Pendergast [71], was originally thought to be a new complex due to its incorrect plotting by the original researchers. We later identified the site using extant archaeological features.

Inflow and exurgence caves occur rarely throughout the greater Las Cuevas area. Besides the previously mentioned inflow associated with Actun P’ook, four other cave entrances of this classification were authenticated. Nearly all were inaccessible due to water flow, collapse, or obstructions of organic material. A single example (Dinosaur Egg Cave), developed into a complex system of large chambers and tunnels following a series of initial constrictions.

5. Conclusions

Most research to date in cave detection utilizes algorithms that search for depressions in local landscape topography, but our hybrid methodology employs both automated and non-automated techniques to find not only sinks, but horizontal cave entrances as well. Using local relief modeling from lidar-derived images, our project was able to identify hundreds of potential cave openings in the Chiquibul Forest Reserve from large sinks to small fissures. We located a wide variety of cave entrances, both vertical and horizontal, ranging from small features that measured less than 1 m in height or diameter to much larger and more easily discovered openings.

In the heavily forested area of the Chiquibul Reserve in western Belize, pedestrian survey is inevitably slow and requires cutting trails and often negotiating rough karstic terrain. Guided by

lidar imagery, our search for cave openings during two six-week summer field seasons, increased our knowledge of confirmed caves in the project area from 4 to 14 sites that were used by the ancient Maya, and an additional 26 unused sites detected in the lidar imagery. We evaluated the accuracy of our lidar detection using two pedestrian survey methods.

Based on other surveys in areas with thick ground cover, the results of our systematic survey were as expected. Using this survey technique, we discovered six karstic features within the domain that were not detected in the lidar image analysis. This is a reminder that that pedestrian survey remains the most reliable method of obtaining the best survey coverage in forested areas. However, it is not the most efficient or cost-effective. Recall that of the 381 survey tiles created for the Las Cuevas surrounds, we were only able to complete 100% pedestrian survey coverage of 10 tiles during two summer field seasons. At this rate, it would take us 74 years to complete the survey!

The results of our opportunistic survey in which we targeted and visited caves detected on the lidar imagery, met with an 86% success rate with only 3 false positives, verifying 26 cave openings. This method proved to be expedient in meeting the project goals of locating and investigating unknown cave sites. We recognize that there will always be cave openings that lidar cannot detect due to intentional or unintentional entrance blockages or thick forest cover, but in terms of heritage preservation, if we are to locate unlooted or relatively intact cave sites in a timely manner, lidar imagery provides the most cost-effective and directly applicable method for detection, far superior to pedestrian survey alone.

Author Contributions: Conceptualization, H.M.; methodology, H.M. and S.M.; investigation H.M. and S.M.; formal analysis, S.M.; resources H.M.; writing—original draft preparation, H.M. and S.M.; writing—review and editing, H.M. and S.M.; visualization, H.M. and S.M.; supervision S.M.; project administration, H.M.; funding acquisition, H.M.

Funding: Funding for the lidar survey was made available from the Alphawood Foundation to the Western Belize Lidar Consortium. The 2017/2018 field seasons were supported by grants to Moyes from the National Geographic Society (#9544-14, GR-000000589) and the Alphawood Foundation.

Acknowledgments: Thanks to the Belize Institute of Archaeology and particularly to John Morris for permitting our research. The survey crew deserves special acknowledgement for their untiring efforts, particularly Nicholas Bourgeois, and our in-country partners Antonio Mai, Javier Mai, and Israel Canto.

Conflicts of Interest: The authors declare no conflict of interest.

References

1. Minty, C.; Bridgewater, S. Introduction. In *A Natural History of Belize: Inside the Maya Forest*; University of Texas Press: Austin, TX, USA, 2012; ISBN 9780292726710.
2. Kidder, A. Five Days over the Maya Country. *Sci. Mon.* **1930**, *30*, 193–205.
3. Saturno, W.; Sever, T.L.; Irwin, D.E.; Howell, B.F.; Garrison, T.G.; Wiseman, J.R.; El-Baz, F. Putting Us on the Map: Remote Sensing Investigation of the Ancient Maya Landscape. In *Remote Sensing in Archaeology*; Wiseman, J., El-Baz, F., Eds.; Springer: New York, NY, USA, 2007; pp. 137–160, ISBN-10: 038744615X.
4. Sever, T.L.; Irwin, D.E. Landscape archaeology: Remote-sensing investigation of the ancient Maya in the Petén rainforest of northern Guatemala. *Anc. Mesoam.* **2003**, *14*, 113–122. [[CrossRef](#)]
5. Blumberg, D.H.; Neta, T.; Margalit, N.; Lazar, M.; Freilikh, V. Mapping exposed and buried drainage systems using remote sensing in the Negev Desert, Israel. *Geomorphology* **2004**, *61*, 239–250. [[CrossRef](#)]
6. Breeze, P.S.; Drake, N.A.; Groucutt, H.S.; Parton, A.; Jennings, R.P.; White, T.S.; Clark-Balzan, L.; Shipton, C.; Scerri, E.M.L.; Stimpson, C.M.; et al. Remote sensing and GIS techniques for reconstructing Arabian palaeohydrology and identifying archaeological sites. *Quart. Int.* **2015**, *382*, 98–119. [[CrossRef](#)]
7. Hritz, C. Contribution of GIS and Satellite-Based Remote Sensing to Landscape Archaeology in the Middle East. *J. Archaeol. Res.* **2014**, *22*, 229–276. [[CrossRef](#)]
8. Parcak, S. Satellite Remote Sensing Methods for Monitoring Archaeological Tells in the Middle East. *J. Field Archaeol.* **2007**, *32*, 65–81. [[CrossRef](#)]
9. Chase, A.F.; Chase, D.Z.; Weishampel, J.F. Lasers in the Jungle: Airborne sensors reveal a vast Maya landscape. *Archaeology* **2010**, *63*, 27–29.

10. Chase, A.F.; Chase, D.Z.; Fisher, C.T.; Leisz, S.; Weishampel, J.F. Geospatial Revolution and Remote Sensing Lidar in Mesoamerican Archaeology. *Proc. Natl. Acad. Sci. USA* **2012**, *109*, 12916–12921. [[CrossRef](#)]
11. Chase, A.F.; Chase, D.Z.; Awe, J.J.; Weishampel, J.F.; Iannone, G.; Moyes, H.; Jaeger, J.; Brown, K.M. The Use of LiDAR in Understanding the Ancient Maya Landscape. *Adv. Archaeol. Pract. A J. Soc. Am. Archaeol.* **2014**, *2*, 208–221. [[CrossRef](#)]
12. Chase, A.F.; Chase, D.Z.; Awe, J.J.; Weishampel, J.F.; Iannone, G.; Moyes, H.; Jaeger, J.; Brown, K.M.; Shrestha, R.; Carter, W.; et al. Ancient Maya Regional Settlement and Inter-Site Analysis: The 2013 West-Central Belize Lidar Survey. *Remote Sens. New Perspect. Remote Sens. Archaeol.* **2014**, *6*, 8671–8695. [[CrossRef](#)]
13. Gallagher, J.M.; Josephs, R.L. Using Lidar to detect cultural resources in a forested environment: An example from Isle Royale National Park, Michigan, USA. *Archaeol. Prospect.* **2008**, *15*, 187–206. [[CrossRef](#)]
14. Hofton, M.A.; Rocchio, L.E.; Blair, J.B.; Dubayah, R. Validation of vegetation canopy lidar sub-canopy topography measurements for a dense tropical forest. *J. Geodyn.* **2002**, *34*, 491–502. [[CrossRef](#)]
15. Weishampel, J.F.; Blair, J.B.; Dubayah, R.; Clark, D.B.; Knox, R.G. Canopy topography of an old-growth tropical rainforest landscape. *Selbyana* **2000**, *21*, 79–87.
16. Weishampel, J.F.; Blair, J.B.; Knox, R.G.; Dubayah, R.; Clark, D.B. Volumetric lidar return patterns from an old-growth tropical rainforest canopy. *Int. J. Remote Sens.* **2000**, *21*, 409–415. [[CrossRef](#)]
17. Sittler, B. Revealing Historical Landscapes by Using Airborne Laser Scanning: A 3-D Model of Ridge and Furrow in Forests near Rastatt, Germany. In Proceedings of the Natscan, Laser-Scanners for Forest and Landscape Assessment—Instruments, Processing Methods and Applications, Freiburg im Breisgau, Germany, 3–6 October 2004; Thies, M., Koch, B., Spiecker, H., Weinacker, H., Eds.; International Archives of Photogrammetry and Remote Sensing: Freiburg im Breisgau, Germany, 2004; Volume XXXVI, Part 8/W2. pp. 258–261.
18. Sherwood, S.C.; Goldberg, P. A Geoarchaeological Framework for the Study of Karstic Cave Sites in the Eastern Woodlands. *Midcont. J. Archaeol.* **2001**, *26*, 145–168.
19. Straus, L.G. Underground Archaeology: Perspectives on Caves and Rockshelters. In *Archaeological Method and Theory*; Schiffer, M.B., Ed.; University of Arizona Press: Tucson, AZ, USA, 1990; Volume 2, pp. 255–304, ISBN 9780120031023.
20. Woodward, J.C.; Goldberg, P. The Sedimentary Records in Mediterranean Rockshelters and Caves: Archives of Environmental Change. *Geoarchaeology* **2001**, *16*, 327–354. [[CrossRef](#)]
21. Moyes, H.; Brady, J.E. Caves as Sacred Space in Mesoamerica. In *Sacred Darkness: A Global Perspective on the Ritual Use of Caves*; Moyes, H., Ed.; University Press of Colorado: Boulder, CO, USA, 2012; pp. 151–170, ISBN 9781607323600.
22. Nicolay, S. Footsteps in the Dark Zone: Ritual Cave Use in Southwest Prehistory. In *Sacred Darkness: A Global Perspective on the Ritual Use of Caves*; Moyes, H., Ed.; University Press of Colorado: Boulder, CO, USA, 2012; pp. 171–184, ISBN 9781607323600.
23. Moyes, H.; Kosakowsky, L.; Ray, E.; Awe, J.J. *The Chronology of Ancient Maya Cave Use in Belize. Research Reports in Belizean Archaeology*; Institute of Archaeology, NICH: Belmopan, Belize, 2017; pp. 327–338.
24. Brown, L. Planting the Bones: Hunting Ceremonialism at Contemporary and Nineteenth-Century Shrines in the Guatemalan Highlands. *Lat. Am. Antiq.* **2005**, *16*, 131–146. [[CrossRef](#)]
25. Scott, A.M. Communicating with the Sacred Earthscape: An Ethnoarchaeological Investigation of Kaqchikel Maya Ceremonies in Highland Guatemala. Ph.D. Dissertation, Department of Anthropology, University of Texas, Austin, TX, USA, 2009.
26. White, W.B.; Culver, D.C. Definition of Cave. In *Encyclopedia of Caves*; White, W.B., Culver, D.C., Eds.; Academic Press: Burlington, MA, USA, 2012; pp. 103–107, ISBN 978-0123838322.
27. Klimchouk, A. Caves. In *Encyclopedia of Caves and Karst Science*; Gunn, J., Ed.; Fitzroy Dearborn: New York, NY, USA, 2004; pp. 417–421, ISBN 9781579583996.
28. Casati, R.; Varzi, A.C. *Holes and Other Superficialities*; MIT Press: Cambridge, MA, USA, 1994; ISBN 9780262032117.
29. Moyes, H.; Montgomery, S. Mapping ritual landscapes using lidar: Cave detection through local relief modeling. *Adv. Archaeol. Pract.* **2016**, *4*, 249–267. [[CrossRef](#)]
30. Rinker, J.N. Airborne infrared thermal detection of caves and crevasses. *Photogramm. Eng. Remote Sens.* **1975**, *44*, 1391–1400. Available online: https://www.asprs.org/wp-content/uploads/pers/1975journal/nov/1975_nov_1391-1400.pdf (accessed on 25 November 2018).

31. Wynne, J.J.; Titus, T.N.; Diaz, D.C. On developing thermal cave detection techniques for earth, the moon and mars. *Earth Planet. Sci. Lett.* **2008**, *272*, 240–250. [[CrossRef](#)]
32. Cooper, A.H. Airborne multispectral scanning of subsidence caused by Permian gypsum dissolution at Ripon, North Yorkshire. *Q. J. Eng. Geol. Hydrogeol.* **1989**, *22*, 219–229. [[CrossRef](#)]
33. Beard, L.P.; Nyquist, J.E.; Carpenter, P.J. Detection of karst structures using airborne EM and VLF. In *SEG Technical Program Expanded Abstracts 1994*; Society of Exploration Geophysicists: Tulsa, OK, USA, 1994; pp. 555–558. [[CrossRef](#)]
34. Gutierrez, F.; Cooper, A.H.; Johnson, K.S. Identification, Prediction, and Mitigation of Sinkhole Hazards in Evaporite Karst Areas. *Environ. Geol.* **2008**, *53*, 1007–1022. [[CrossRef](#)]
35. Kobal, M.; Bertoncelj, I.; Pirotti, F.; Dakskobler, I.; Kutnar, L. Using Lidar Data to Analyse Sinkhole Characteristics Relevant for Understory Vegetation under Forest Cover—Case Study of a High Karst Area in the Dinaric Mountains. *PLoS ONE* **2015**, *10*, e0122070. [[CrossRef](#)] [[PubMed](#)]
36. Miao, X.; Qiu, X.; Wu, S.S.; Luo, J.; Gouzie, D.R.; Xie, H. Developing efficient procedures for automated sinkhole extraction from lidar DEMs. *Photogramm. Eng. Remote Sens.* **2013**, *79*, 545–554. [[CrossRef](#)]
37. Wu, Q.; Deng, C.; Chen, Z. Automated delineation of karst sinkholes from LiDAR-derived digital elevation models. *Geomorphology* **2016**, *266*, 1–10. [[CrossRef](#)]
38. Weishampel, J.F.; Hightower, J.N.; Chase, A.F.; Chase, D.Z.; Patrick, R.A. Lidar Detection and Characterization of Karst Depressions. *J. Cave Karst Stud.* **2011**, *3*, 187–196. [[CrossRef](#)]
39. Weishampel, J.F.; Hightower, J.N.; Chase, A.F.; Chase, D.Z. Remote sensing of below-canopy land use features from the Maya polity of Caracol. In *Understanding Landscapes: From Discovery through Land Their Spatial Organization*; Caracol Archaeological Project, Department of Anthropology, University of Las Vegas: Las Vegas, NV, USA, 2013; pp. 131–136. Available online: <http://www.caracol.org/wp-content/uploads/2016/05/WeishampelEtAl2013.pdf> (accessed on 12 November 2018).
40. Zhu, J.; Taylor, T.P.; Currans, J.C.; Crawford, M.M. Improved Karst Sinkhole Mapping in Kentucky using LiDAR Techniques: A Pilot Study in Floyds Fork Watershed. *J. Cave Karst Stud.* **2014**, *76*, 207–216. [[CrossRef](#)]
41. Awe, J.J. The Western Belize Regional Cave Project: Objectives, Context, and Problem Orientation. In *The Western Belize Regional Cave Project: A Report of the 1997 Field Season*; Awe, J.J., Ed.; University of New Hampshire, Department of Anthropology Occasional: Durham, NH, USA, 1998; pp. 1–22.
42. Moyes, H. Cluster Concentrations, Boundary Markers, and Ritual Pathways: A GIS Analysis of Artifact Cluster Patterns at Actun Tunichil Muknal, Belize. In *The Maw of the Earth Monster: Mesoamerican Ritual Cave Use*; Brady, J.E., Prufer, K.M., Eds.; University of Colorado Press: Boulder, CO, USA, 2005; pp. 269–300, ISBN-13: 9780292705869.
43. Moyes, H.; Awe, J.J.; Brook, G.; Webster, J. The Ancient Maya Drought Cult: Late Classic Cave Use in Belize. *Lat. Am. Antiq.* **2009**, *20*, 175–206. [[CrossRef](#)]
44. Colas, P.R.; Reeder, P.; Webster, J. The Ritual Use of a Cave on the Northern Vaca Plateau, Belize, Central America. *J. Cave Karst Stud.* **2000**, *62*, 6–10.
45. Moyes, H.; Robinson, M.; Voorhies, B.; Kosakowsky, L.; Arksey, M.; Ray, E.; Hernandez, S. *Dreams at Las Cuevas: A Location of High Devotional Expression of the Late Classic Maya*; Research Reports in Belizean Archaeology; Institute of Archaeology, NICH: Belmopan, Belize, 2015; Volume 12, pp. 239–249.
46. Bridgewater, S. *A Natural History of Belize: Inside the Maya Forest*; University of Texas Press: Austin, TX, USA, 2012; pp. 96–99, ISBN 9780292726710.
47. Bateson, J.H.; Hall, I.H.S. *The Geology of the Maya Mountains, Belize*; HM Stationery Office, London.: London, UK, 1977; Volume 3, ISBN 978-0118807654.
48. Miller, T.E. Geologic and hydrologic controls on karst and cave development in Belize. *J. Cave Karst Stud.* **1996**, *58*, 100–120.
49. Vinson, G.L. Upper Cretaceous and Tertiary Stratigraphy in Guatemala. *Bull. Am. Assoc. Petr. Geol.* **1962**, *46*, 425–465.
50. Miller, T.E. Inside Chiquibul. *Natl. Geogr.* **2000**, *197*, 54–71.
51. Feld William, A. The Caves of Caracol: Initial Impressions. In *Studies in the Archaeology of Caracol, Belize*; Chase, D.Z., Chase, A.F., Eds.; Pre-Columbian Art Research Institute Monograph 7; PARI: San Francisco, CA, USA, 1994; pp. 76–82.
52. Reeder, P.; Brinkmann, R.; Alt, E. Karstification on the northern Vaca plateau, Belize. *J. Cave Karst Stud.* **1996**, *58*, 121–130.

53. Benson, R.C.; Yuhr, L.B. *Site Characterization in Karst and Pseudokarst Terraines: Practical Strategies and Technology for Practicing Engineers, Hydrologists and Geologists*; Springer: New York, NY, USA, 2015; pp. 16–25, ISBN 9789401799232.
54. Williams, P.; Gunn, J. Dolines. In *The Encyclopedia of Caves and Karst Science*; Gunn, J., Ed.; Fitzroy Dearborn: New York, NY, USA, 2003; pp. 304–310, ISBN 9781579583996.
55. Gatzilis, D.; Andersen, H.E. *A Guide to LIDAR Data Acquisition and Processing for the Forests of the Pacific Northwest*; Gen. Tech. Rep. PNW-GTR-768; US Department of Agriculture, Forest Service, Pacific Northwest Research Station: Portland, OR, USA, 2008; p. 768, ISBN 9781508770954. Available online: https://www.fs.fed.us/pnw/pubs/pnw_gtr768.pdf (accessed on 19 November 2018).
56. Kokalj, Z.; Hesse, R. *Airborne Laser Scanning Raster Data Visualization—A Guide to Good Practice*; Založba ZRC: Ljubljana, Slovenia, 2017; ISBN 9789612549848.
57. Brassel, K.E.; Little, J.; Peucker, T.K. Automated Relief Representation. *Ann. Assoc. Am. Geogr.* **1974**, *64*, 610–611. Available online: <https://www.jstor.org/stable/2569517> (accessed on 19 November 2018).
58. Zakšek, K.; Oštir, K.; Kokalj, Ž. Sky-View Factor as a Relief Visualization Technique. *Remote Sens.* **2011**, *3*, 398–415. [CrossRef]
59. Yokoyama, R.; Shirasawa, M.; Pike, R.J. Visualizing topography by openness: A new application of image processing to digital elevation models. *Photogramm. Eng. Remote Sens.* **2002**, *68*, pp. 257–266. Available online: <https://pdfs.semanticscholar.org/c3d9/a561fdb9e8c34a2b79152aea72b46090bb2e.pdf> (accessed on 19 November 2018).
60. Hesse, R. Visualisierung Hochauflösender Digitaler Geländemodelle Mit LiVT. In *Computeranwendungen Und Quantitative Methoden in Der Archäologie. 4*; Workshop Der AG CAA 2013; Lieberwirth, U., Herzog, I., Eds.; Berlin Studies of the Ancient World: Berlin, Germany, 2016; pp. 109–128.
61. Doctor, D.H.; Young, J.A. An Evaluation of Automated GIS Tools for Delineating Karst Sinkholes and Closed Depressions from 1-m LiDAR Derived Digital Elevation Data. In Proceedings of the 13th Multidisciplinary Conference on Sinkholes and the Engineering and Environmental Impacts of Karst, NCKRI SYMPOSIUM 2, Carlsbad, NM, USA, 6–10 May 2013; Land, L., Doctor, D.H., Stephenson, J.B., Eds.; National Cave and Karst Research Institute: Carlsbad, NM, USA, 2013; pp. 449–458.
62. Hesse, R. LiDAR-derived Local Relief Models—A new tool for archaeological prospection. *Archaeol. Prospect.* **2010**, *17*, 67–72. [CrossRef]
63. Novák, D. Local Relief Model (LRM) Toolbox for ArcGIS. Electronic Document. 2014. Available online: http://www.academia.edu/5618967/Local_Relief_Model_LRM_Toolbox_for_ArcGIS_UPDATE_2014-10-7 (accessed on 12 November 2018).
64. Hare, T.; Masson, M.; Russell, B. High-Density LiDAR Mapping of the Ancient City of Mayapan. *Remote Sens.* **2014**, *6*, 9064–9085. [CrossRef]
65. Hutson, S.R. Adapting LiDAR Data for Regional Variation in the tropics: A case study from the Northern Maya Lowlands. *J. Archaeol. Sci.* **2015**, *4*, 252–263. [CrossRef]
66. Prufer, K.M.; Thompson, A.E.; Kennett, D.J. Evaluating Airborne LiDAR for Detecting Settlements and Modified Landscapes in Disturbed Tropical Environments at Uxbenka, Belize. *J. Archaeol. Sci.* **2015**, *57*, 1–13. [CrossRef]
67. Reese-Taylor, K.; Hernández, A.A.; Esquivel, F.C.A.F.; Monteleone, K.; Uriarte, A.; Carr, C.; Acuña, H.G.; Fernandez-Diaz, J.C.; Peuramaki-Brown, M.; Dunning, N. Boots on the Ground at Yaxnohcah: Ground-Truthing Lidar in a Complex Tropical Landscape. *Adv. Archaeol. Pract.* **2016**, *4*, 314–338. [CrossRef]
68. Yaeger, J.; Brown, M.J.; Cap, B. Locating and Dating Sites Using Lidar Survey in a Mosaic Landscape in Western Belize. *Adv. Archaeol. Pract.* **2016**, *4*, 339–356. [CrossRef]
69. Rosenswig, R.M.; López-Torrijos, R.; Antonelli, C.E.; Mendelsohn, R.R. Lidar Mapping and Surface Survey of the Izapa State on the Tropical Piedmont of Chiapas, Mexico. *J. Archaeol. Sci.* **2013**, *40*, 1493–1507. [CrossRef]
70. Crow, P.; Benham, S.; Devereux, B.J.; Amable, G.S. Woodland Vegetation and Its Implications for Archaeological Survey Using LiDAR. *Forestry* **1989**, *80*, 241–252. [CrossRef]
71. Pendergast, D.M. *Excavations at Eduardo Quiroz Cave, British Honduras (Belize)*; Toronto, Royal Ontario Museum, Art and Archaeology Occasional: Toronto, ON, Canada, 1971.

